Tracing the fluid source of heavy REE mineralisation in carbonatites using a novel method of oxygen-isotope analysis in apatite: The example of Songwe Hill, Malawi

Sam Broom-Fendley [a,b,*], Timothy Heaton [c], Frances Wall [a], Gus Gunn [b]

[a] Camborne School of Mines, University of Exeter, Penryn Campus, Cornwall TR10 9FE, United Kingdom
[b] British Geological Survey, Nicker Hill, Keyworth, Nottingham NG12 5GD, United Kingdom
[c] NERC Isotope Geosciences Laboratory, British Geological Survey, Nicker Hill, Keyworth, Nottingham NG12 5GG, United Kingdom

ABSTRACT

Stable (C and O) isotope data from carbonates are one of the most important methods used to infer genetic processes in carbonatites. However despite their ubiquitous use in geological studies, it is suspected that carbonates are susceptible to dissolution-reprecipitation and isotopic resetting, especially in shallow intrusions, and may not be the best records of either igneous or hydrothermal processes. Apatite, however, should be much less susceptible to these resetting problems but has not been used for O isotope analysis. In this contribution, a novel bulk-carbonatite method for the analysis of O isotopes in the apatite PO_4 site demonstrates a more robust record of stable isotope values. Analyses of apatite from five carbonatites with magmatic textures establishes a preliminary Primary Igneous Apatite (PIA) field of $\delta^{18}O = +2.5$ to $+6.0‰$ (VSMOW), comparable to Primary Igneous Carbonatite (PIC) compositions from carbonates.

Carbonate and apatite stable isotope data are compared in 10 carbonatite samples from Songwe Hill, Malawi. Apatite is heavy rare earth element (HREE) enriched at Songwe and, therefore, oxygen isotope analyses of this mineral are ideal for understanding HREE-related mineralisation in carbonatites. Carbonate C and O isotope ratios show a general trend, from early to late in the evolution, towards higher $\delta^{18}O$ values ($+7.8$ to $+26.7‰$, VSMOW), with a slight increase in $\delta^{13}C$ (-4.6 to $-0.1‰$, VPDB). Oxygen isotope ratios from apatite show a contrary trend, decreasing from a PIA field towards more negative values ($+2.5$ to $-0.7‰$, VSMOW). The contrasting results are interpreted as the product of the different minerals recording fluid interaction at different temperatures and compositions. Modelling indicates the possibility of both a CO_2 rich fluid and mixing between meteoric and deuteric waters. A model is proposed where brecciation leads to depressurisation and rapid apatite precipitation. Subsequently, a convection cell develops from a carbonatite, interacting with surrounding meteoric water. REE are likely to be transported in this convection cell and precipitate owing to decreasing salinity and/or temperature.

1. Introduction

Stable C and O isotope ratios are powerful tools for investigating the evolution of carbonatites, allowing interpretation of either crystallisation temperature (e.g. Haynes et al., 2003; Demény et al., 2004a) or fluid

composition and evolution (e.g. Andersen, 1987; Santos and Clayton, 1995; Andrade et al., 1999; Zaitsev et al., 2002; Downes et al., 2014; Moore et al., 2015; Trofanenko et al., 2016). Interpretation of most carbonatite C and O isotope data revolves around a range of values for 'Primary Igneous Carbonatites' (PIC), where 'primary' denotes analyses of material unaffected by weathering or by hydrothermal alteration. Published values for PIC vary, the earliest documented being $\delta^{13}C = -5.0$ to $-8.0‰$ and $\delta^{18}O = +6.0$ to $+8.5$ (vs VPDB and VSMOW, respectively, throughout the manuscript), based on a similar range of values for fresh samples from multiple complexes (Taylor et al., 1967). Slightly different ranges have been suggested by later authors (Deines, 1989; Keller and Hoefs, 1995; Demény et al., 2004b; Jones et al., 2013) and in this contribution the field of Jones et al. (2013) is utilised throughout. These ranges and the effects of different processes on the C and O isotope

composition of carbonatites are summarised in Fig. 1. The processes affecting the isotope composition include:

1) **Rayleigh fractionation**, where calcite crystallises in equilibrium with H_2O and CO_2 from a fluid/magma, leading to increasing $\delta^{13}C$ and $\delta^{18}O$ in subsequently crystallised carbonates (Deines, 1970, 1989; Ray and Ramesh, 2000)

2) **Sediment** incorporation, which typically increases $\delta^{13}C$ and $\delta^{18}O$ (Demény and Harangi, 1996; Demény et al., 1998).

3) **Degassing**, attributed to carbonatites which have lower $\delta^{13}C$ than PIC through preferential partitioning of heavy carbon into the gas phase (Suwa et al., 1975; Demény et al., 1994). Modelling indicates that this can be accompanied by a corresponding decrease in $\delta^{18}O$ values which becomes more extreme as the temperature of degassing decreases from 500 to 100 °C (Santos and Clayton, 1995).

4) **Post-magmatic (secondary) alteration**, involving interaction with fluid after the carbonatite is emplaced in the crust. The nature and effect of the interaction between carbonatite and a fluid is dictated by the fluid composition, temperature and chemistry. Three fluids with which a carbonatite may interact include:

  a. **Seawater**, although this rarely influences carbonatites because they are generally emplaced in stable continental locations (Woolley and Kjarsgaard, 2008).

  b. **Deuteric water**, which is assumed to have the same initial $\delta^{18}O$ as PIC. Exchange with deuteric water can raise the $\delta^{18}O$ of a carbonatite with which it interacts, depending on temperature and composition. If the fluid is around 100 °C then $\delta^{18}O$ values of up to 25‰ can be attained (Deines, 1989; Santos and Clayton, 1995; Ray and Ramesh, 1999).

  c. **Meteoric water**, which generally has a negative $\delta^{18}O$ value (Hoefs, 2008), and a negligible carbon content (except where it has previously interacted with sedimentary carbonate). Exchange with meteoric water below approximately 200 °C results in increased $\delta^{18}O$ in the carbonatite, whereas exchange at temperatures higher than this results in ^{18}O depletion (Deines, 1989).

Post-magmatic fluids are an important factor in carbonatite-derived rare earth element (REE) mineralisation, especially in near-surface intrusions (Deines and Gold, 1973). Typically, REE mineralisation associated with carbonatites is light (L)REE-rich, although heavy (H)REE-rich exceptions are known (e.g. Wall et al., 2008; Broom-Fendley et al., 2016a,b). Where LREE mineralisation has occurred, C and O isotope ratios invariably extend beyond the PIC field, typically to higher $\delta^{18}O$ and $\delta^{13}C$ values, generally associated with post-magmatic fluids (Andrade et al., 1999; Zaitsev et al., 2002; Marks et al., 2009; Downes et al., 2014; Moore et al., 2015; Trofanenko et al., 2016). This trend is similarly followed at the HREE-enriched Lofdal carbonatite, Namibia

(Do Cabo, 2014). Most C and O analyses, however, are from carbonates which can easily be re-crystallised, even at low temperatures (Malone et al., 1996; Chakhmouradian et al., 2016). Where multiple fluids have interacted with a carbonatite, isotopic resetting can occur and it may not be possible to confidently associate the fluids leading to REE mineralisation with carbonate C and O isotope ratios. For example, at the Kangankunde carbonatite, Malawi, dolomite reaches $\delta^{18}O$ values in excess of 20‰ higher than in strontianite associated with REE mineralisation, with the $\delta^{18}O$ increase corresponding to 'darker' mineral grains representative of increased alteration (Wall, 2000).

Apatite is a relatively resistant mineral to dissolution-reprecipitation and is effectively closed to isotopic diffusion below 550 °C (Cole and Chakraborty, 2001). C and O isotopes can be measured in apatite because CO_3^{2-} substitutes into the PO_4 and F/Cl/OH site (Nadeau et al., 1999; Pan and Fleet, 2002; Yi et al., 2013). However, for oxygen isotope analysis, oxygen from the PO_4 site is normally isolated as it is the least susceptible to isotopic exchange (O'Neil et al., 1994; Vennemann et al., 2002; Kohn and Cerling, 2002). Biogenic apatite is commonly analysed for modern ecological studies (e.g. Kohn and Cerling, 2002) and for palaeotemperature studies (e.g. using fish teeth, Kolodny et al., 1983; Lécuyer et al., 2003; phosphorites, Shemesh et al., 1983, 1988; and mammalian teeth, Grimes et al., 2008). There have been, however, few studies of oxygen isotopes in phosphates from igneous or hydrothermal rocks. These are restricted to granites (Farquhar et al., 1993; Burmann et al., 2013), meteorites (Greenwood et al., 2003), pyromorphite deposits (Burmann et al., 2013) and limited studies in carbonatites (Conway and Taylor, 1969; Santos and Clayton, 1995; Tichomirowa et al., 2006). The latter are from samples which are, texturally, primary magmatic carbonatites and range in composition between $\delta^{18}O$ = +4.2 to +5.7‰ (Fig. 2). However, they are analyses of O from all the O sites in apatite, rather than isolating PO_4-O.

Despite the limited number of studies, apatite is a good mineral to determine the O-isotope composition of carbonatites. Advantages include its ubiquity, apatite typically comprises 2–5% of a carbonatite (Hogarth, 1989); its occurrence throughout different stages of carbonatite evolution, although it is commonly an early-crystallising mineral (Kapustin, 1980); and, at some carbonatites, elevated HREE concentrations have been identified in late-stage apatite (e.g. Songwe and Tundulu, Malawi; Broom-Fendley et al., 2016a,b). It is, therefore, a mineral with good potential for: (1) evaluating the changing O-isotope composition of carbonatites during their evolution, including crystallisation from low temperature, post-magmatic, fluids; and (2) understanding the role of post-magmatic fluids for HREE-enriched apatite mineralisation. In this contribution a method for analysing $\delta^{18}O$ in the apatite PO_4 site ($\delta^{18}O_{PO_4}$) is developed and tested to expand our understanding of these two points.

2. Sample selection and hypotheses

Samples were selected from five globally-distributed carbonatites with magmatic crystallisation textures and from different paragenetic
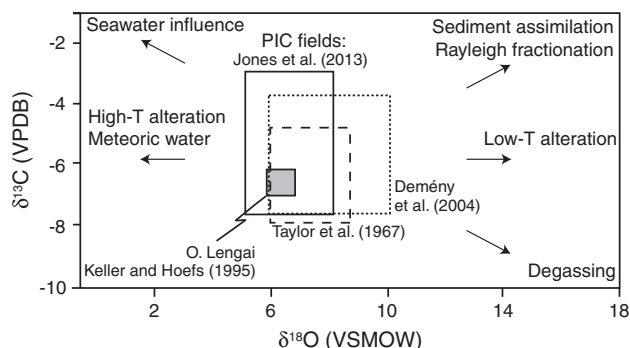

Fig. 1. The principal controls on carbonatite O and C isotope ratios after Demény et al. (2004b) and Deines (1989). Primary carbonatite fields from Taylor et al. (1967); Keller and Hoefs (1995); Demény et al. (2004b) and Jones et al. (2013).
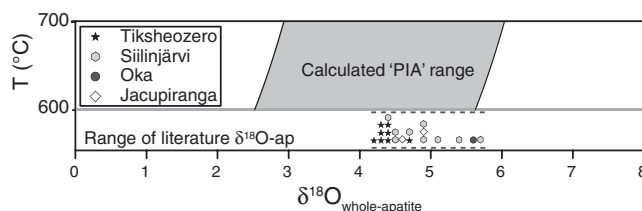

Fig. 2. Compilation of previous O-isotope analyses of apatite from Oka (Conway and Taylor, 1969), Jacupiranga (Santos and Clayton, 1995), Tiksheozero, and Siilinjärvi (Tichomirowa et al., 2006), plotted against an estimated PIA a range using the PIC range (+5.3 to +8.4‰) and the fractionation factor from Fortier and Lüttge (1995) for the temperatures 600–700 °C.

stages of the Songwe Hill carbonatite, Malawi. Samples from the primary magmatic carbonatites were selected to test the validity of measuring $\delta^{18}O_{PO_4}$ while samples from Songwe were used to attempt to fingerprint changing fluid conditions leading to HREE mineralisation.

2.1. Primary magmatic carbonatites

Five samples from carbonatites with a magmatic crystallisation texture were acquired from the following well-studied carbonatites: Oka and St Honoré, Canada (Vallée and Dubuc, 1970; Gold et al., 1986; Deines, 1970, 1989); Jacupiranga, Brazil (Melcher, 1966; Morbidelli et al., 1995; Santos and Clayton, 1995; Costanzo et al., 2006); Fen, Norway (Barth and Ramberg, 1966; Andersen, 1987), and Kaiserstuhl, Germany (Wimmenauer, 1966; Hubberten et al., 1988; Keller, 1981; Table 1). These samples were selected to understand (1) if $\delta^{18}O_{PO_4}$ values from magmatic carbonatites fall within a limited field (PIA) and (2) to confirm that $^{18}O_{PO_4}$ is not susceptible to diffusion and isotopic resetting when interacting with a hydrothermal fluid.

To test if magmatic carbonates fall in a limited $\delta^{18}O_{PO_4}$ range, samples from Oka, Jacupiranga, Fen, and Kaiserstuhl were selected as previously published carbonate C and O data for these carbonatites falls into, or very close to, the PIC box (Fig. 3). Furthermore, apatite $\delta^{18}O$ values from Oka and Jacupiranga have previously been published. Isotope ratios from apatite in these samples can be compared to calcite data (considered as PIC) to check if a range for PIA is comparable with apatite–calcite fractionation factors (Fortier and Lüttge, 1995).

A sample from the St Honoré carbonatite, Canada, was analysed to interpret if apatite $\delta^{18}O_{PO_4}$ is susceptible to diffusion when interacting with a hydrothermal fluid. Oxygen isotope data from St Honoré spans a wide range in carbonate $\delta^{18}O$ (Fig. 3), interpreted as a result of interaction of different fluid stages (Deines, 1989). Cathodoluminescence images of sample StH-2 (analysed in this study) clearly show two calcite generations (cal-1 and cal-2), with cal-2 growing between cleavage planes in biotite, and incurring into magnetite grains (Fig. 4). These textures are indicative of interaction between the early carbonatite and a late fluid. Apatite grains, however, appear petrographically unaffected.
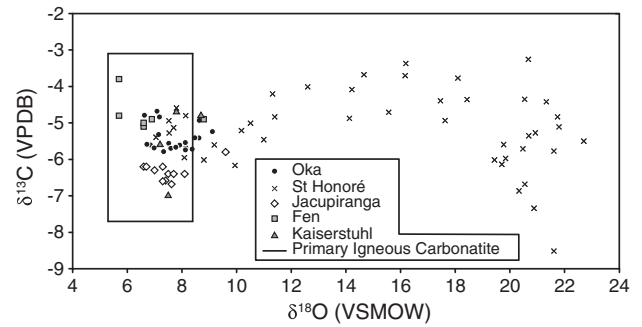

Fig. 3. Carbonatite C and O analyses from Oka (Deines, 1989; Haynes et al., 2003), St Honoré (Deines, 1989), Jacupiranga (Morikiyo et al., 1990; Santos and Clayton, 1995; Haynes et al., 2003), Fen (Andersen, 1987), and Kaiserstuhl (Hubberten et al., 1988). Included for reference is the PIC field after Jones et al. (2013).

2.2. Songwe carbonatite

The Songwe Hill carbonatite is a Lower Cretaceous, shallowly emplaced, multi-stage carbonatite located in the Chilwa Alkaline Province, Malawi (Garson, 1965; Broom-Fendley et al., 2016c). It comprises four separate carbonatite stages (C1–4), progressively increasing in REE content. Minor coarse-grained calcite carbonatite, present as clasts, has a distinct magmatic texture (C1), but most carbonatite at Songwe comprises fine-grained calcite carbonatite (C2) and ferroan calcite carbonatite (C3) incorporating a significant component of fenite clasts. Post-magmatic apatite-fluorite veins (C4) and Mn-Fe veins cross-cut carbonatite and represent late stages of mineralisation and fluid alteration. Songwe is predominantly a LREE deposit, with an established (NI 43-101 compliant) probable mineral reserve of 8.4 million tonnes at 1.6% total rare earth oxide (TREO) (Croll et al., 2014). However, a particular feature is the substantial amount of the HREE contained in apatite (Broom-Fendley et al., 2016b), which is planned to be a co-product of the LREE ore mineral, synchysite-(Ce). Multiple apatite types can be distinguished, texturally and geochemically, ranging from (Broom-Fendley et al., 2016b; Fig. 5):

Table 1
Sample details, mineralogy and stable isotope data.

Songwe samples									
Sample	Rock type	Ap type	Mineralogy	Whole rock			Apatite separate	Whole rock	
				% PO$_4$	$\delta^{18}O_{PO_4}$[a]	$\delta^{18}O_{PO_4}$[b]	$\delta^{18}O_{PO_4}$[a]	$\delta^{13}C_{CO_3}$	$\delta^{18}O_{CO_3}$
T0178	C4	4	ap, flr, cc, Ksp, xnt, syn	27	−0.7	−0.9		−0.1	+26.7
T0232	C2	3	ap, cc, ank, flr, MnO	2		+2.9		−4.0	+19.8
T0250	C2	3	cc, gth, ap, ank					−4.0	+19.7
T0167	C3	3	ap, flr, ank, str, syn	12	+1.1	+1.6			
T0202	C2	3	Ksp, ap, zrc, cc, gth	0.3	+1.9			−3.7	+10.0
T0206	C1	1,2,(3)	ap, zrc, cc, Ksp, py	1	+2.2 (±0.25)			−3.4	+7.8
T0218	C1	1,2	ap, zrc, cc, ank, gth, Ksp	0.2	+2.5			−4.3	+14.0
T0225	C2	3	ap, cc, ank, flr, MnO	5	+1.7 (±0.17)			−4.6	+12.7
T0262	C2	3	ap, cc, Ksp, pyro, py, zrc	18	+1.5 (±0.05)			−2.5	+19.6
T0227	Mn-Fe-vein	3	ap, gth	26	+3.0	+2.8			

Globally-distributed, primary magmatic carbonatite samples								
Sample	Location	Mineralogy	Whole rock			Apatite separate	Whole rock	
			% PO$_4$	$\delta^{18}O_{PO_4}$[a]	$\delta^{18}O_{PO_4}$[b]	$\delta^{18}O_{PO_4}$[a]	$\delta^{13}C_{CO_3}$	$\delta^{18}O_{CO_3}$
Fen 202/76	Fen, Norway	cc, ap, mt, bt	3	+4.1		+4.7	−4.8	+7.7
Jaq-12	Jacupiranga, Brazil	cc, ap	29	+5.4 (±0.11)		+5.2	−6.3	+8.0
K-Stuhl	Kaiserstuhl, Germany	cc, ap, mt, bt	2	+5.0			−6.6	+8.2
OKA-1	Oka, Canada	cc, ap, mt, bt, pyro	3	+5.3		+5.3	−4.5	+7.7
StH-2	St Honoré, Canada	cc, ap, mt, bt, pyro	10	+4.6 (±0.04)		+4.4	−5.5	+16.4

Notes: cc, calcite; ap, apatite; mt, magnetite; bt, biotite; pyro, pyrochlore; zrc, zircon; ank, ankerite; gth, goethite; Ksp, K-feldspar; py, pyrite; MnO, Mn-oxide minerals; flr, fluorite; str, strontianite; syn, synchysite-(Ce); xnt, xenotime-(Y). Refer to text for C1–4 stages.

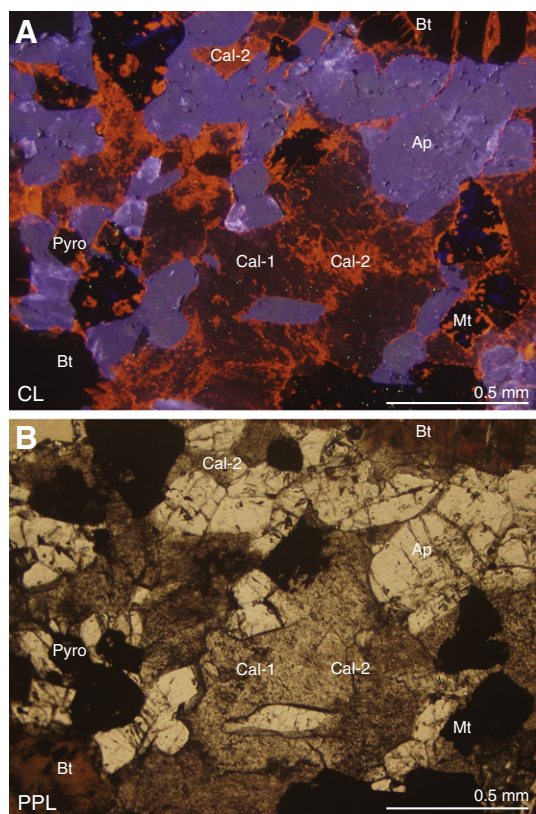[a] 'ML-ON' method.
[b] 'Tooth' method.

Fig. 4. Cathodoluminescence (A) and plane-polarised light (B) images of carbonate recrystallisation at the St Honoré carbonatite (STH-2). Remnant rhombohedra of cal-1 are overprinted by later cal-2. Cal-2 also overprints magnetite (mt), pyrochlore (pyro) and biotite (bt) while apatite (ap) appears unaffected.

1. **Ap-1**, early, ovoid, LREE-rich, magmatic apatite in C1 calcite carbonatite (samples T0218 and T0206).
2. **Ap-2**, slightly HREE-enriched overgrowths on Ap-1 in calcite carbonatite (rims on samples T0218 and T0206).
3. **Ap-3**, late, anhedral, HREE-rich, hydrothermal apatite in C2 calcite carbonatite (samples T0202, T0232, T0225, T0250 and T0262); (C3) ferroan calcite carbonatite (T0167); and Mn-Fe-veins (T0227).
4. **Ap-4**, late, anhedral, HREE-rich, hydrothermal apatite associated with fluorite and minor xenotime from apatite-fluorite veins (C4) (Sample T0178).

Late-stage, HREE-rich, apatite (ap-3 and ap-4) is likely to have formed under hydrothermal conditions. Evidence for this includes the cross-cutting nature of many of the apatite 'stringers' as well as a negative yttrium anomaly in the apatite REE distribution (Broom-Fendley et al., 2016b; Fig. 5B). Furthermore, apatite fluid-inclusion homogenisation temperatures are low, between 200 and 350 °C, with a minimum crystallisation temperature of 160 °C constrained by fluid inclusions in fluorite. The late hydrothermal conditions at Songwe could be from a fluid exsolved from the carbonatite or from interaction with local meteoric fluids. To understand more about the, potentially unique, formation of HREE-enriched apatite at Songwe, samples were selected to test:

1. Are there variations in isotope ratios at Songwe, and can these be related to Rayleigh fractionation, fluid alteration or sediment assimilation?
2. Can the fluid inclusion data be tied with the isotope data to determine the conditions of the mineralising fluid?
3. Can carbonate and apatite data be reconciled into a general model of fluid evolution?

A list of the samples and their mineralogy from Songwe is shown in Table 1. Apatite-rich samples were selected from different paragenetic stages and with different apatite REE distributions (Fig. 5). Samples with fluid inclusion data were selected to tie together homogenisation temperatures, as a proxy for crystallisation temperatures, with isotope data to obtain information on the isotopic composition of the mineralising fluid.

3. Methods

3.1. Sample preparation

Whole-rock samples were prepared by crushing carbonatite rock and grinding to a fine powder using a tungsten carbide TEMA mill. Crystals of pure apatite were separated from a few carbonatites by crushing, sieving, removing carbonate by dissolution in 20% acetic acid at 50 °C for 72 h (a process known not to affect apatite $\delta^{18}O$ values; Koch et al., 1997; Garvie-Lok et al., 2004), and hand picking. The apatite crystals were then ground in a steel mortar and pestle.

3.2. Carbonate $\delta^{13}C$ and $\delta^{18}O$ analyses

Whole rock powders were reacted offline in vacuo with 100% phosphoric acid at 16 °C for 1 h to ensure dissolution of calcite only (Dean et al., 2015). The liberated CO_2 was cryogenically purified before transfer to a VG Optima dual-inlet mass spectrometer (VG Isotopes, Winsford, England), and the calcite $\delta^{13}C$ and $\delta^{18}O$ values versus VSMOW determined by comparison with identically treated standards calibrated against NBS 18 and NBS 19. Duplicate analyses of samples differed by $<\pm 0.2\permil$ for $\delta^{13}C$ and $\delta^{18}O$.

3.3. Silver phosphate preparation

Whole rock powders were first tested for approximate phosphate content, and the presence of any arsenate. Samples were dissolved in 3 M HCl, pH adjusted to near neutral, and the solutions tested for phosphate using method 8048 with colorimeter DR/890, and arsenate using an EZ Arsenic Test Kit (all HACH Company, Loveland, USA).

3.3.1. ML-ON method
Preparation of silver phosphate followed a method modified from those of McLaughlin et al. (2004) and O'Neil et al. (1994) (ML-ON method). For whole rock powders, 2 M HNO_3 was added to enough powder (based on the measured phosphate content) to yield at least 10 mg of silver phosphate; with the amount of acid being just sufficient to ensure that the pH was below 2 after all reactive carbonate had been dissolved. For apatite separates, 2 mL 2 M HNO_3 was added to 10 mg of apatite. After adding an amount of water 10 times the volume of acid used, the solution was separated, mixed with cation resin (2 mL Dowex 50W-X8, NO_3 form, per 10 mL solution), and shaken overnight. The solution was separated by filtration, its pH raised to pH 2–3 with drops of 5 M KOH, and 5 mL 1 M $MgCl_2 \cdot 6H_2O$ added, followed by a further 1 mL 5 M KOH to form a magnesium hydroxide flocculant. The next stages, treating the resulting flocculant, and the formation and separation of cerium phosphate, broadly followed the method of McLaughlin et al. (2004) up to the stage where the solution was separated from the anion resin after removal of the cerium. Following O'Neil et al. (1994) an ammoniacal silver nitrate solution was then added, with ammonia in sufficient excess to raise the pH about 10, and the silver phosphate crystals were then formed slowly by heating the alkaline mixture (70 °C for several hours) until all phosphate was precipitated and the final pH was neutral (near pH 7). Crystals were recovered by filtering on 0.2 μm polycarbonate membranes, washed several times with water, dried at 70 °C, weighed, and lightly ground/homogenised in a steel mortar.
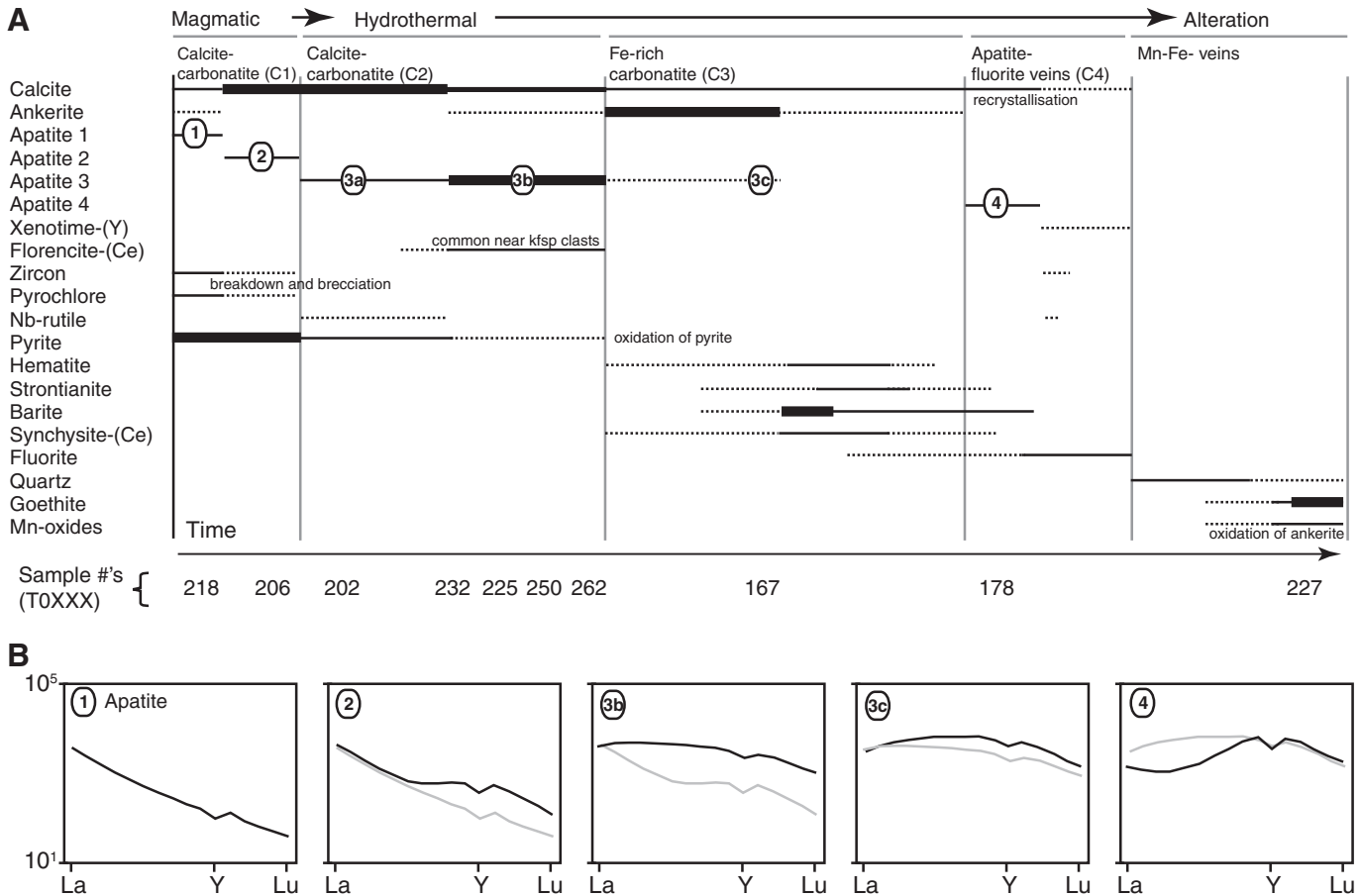
Fig. 5. (A) Paragenesis of the Songwe Hill carbonatite after Broom-Fendley et al. (2016b), with approximate position of the samples selected for isotope analysis. (B) Median REE distributions of different apatite generations. Grey lines represent the distribution of the previous apatite generation for reference. Circled numbers also correspond to stages in Fig. 10.

3.3.2. Tooth enamel method

As a comparison, silver phosphate was prepared from a few whole rock samples using a different method commonly employed for separating phosphate from tooth enamel (Chenery et al., 2012 based on O'Neil et al., 1994). This method is simpler, but not suited to samples with low phosphate concentrations.

3.4. Phosphate $\delta^{18}O$ analysis

Silver phosphate samples and standards were weighed to between 380 and 420 µg in silver capsules and placed in a Zero Blank Autosampler (Costech Analytical Technologies, Valencia, USA) atop a TC/EA (Thermal Conversion/Elemental Analyser; ThermoFinnigan, Bremen, Germany) containing graphite at 1400 °C. Carbon monoxide, produced by thermal decomposition of the phosphate in the presence of the graphitic carbon, was passed in a stream of helium through a Conflo-III into a Delta + XL mass spectrometer (both ThermoFinnigan, Bremen, Germany) where the $^{18}O/^{16}O$ ratios were compared to those of a reference gas and an internally run silver phosphate laboratory standard. $\delta^{18}O$ values versus VSMOW are based on calibrating the laboratory standard against a silver phosphate reference material. In the absence of an agreed international reference material we utilised silver phosphate standard 'B2207' (supplied by Elemental Microanalysis Ltd., Okehampton, England) which has been measured in an inter-laboratory comparison study to have a certified $\delta^{18}O$ value of 21.7‰ (VSMOW). All samples were run in triplicate, with a typical precision of $1\sigma \leq 0.3‰$.

4. Results

4.1. Silver phosphate preparation

Arsenic was not detected in any of the whole rock powders, suggesting that As levels were below 3 ppm. This figure is supported by As levels in Songwe apatite, determined by LA ICP MS, which are <20 ppm (Broom-Fendley et al., 2016b). We would, therefore, not expect our results to be compromised by contamination with silver arsenate (Burmann et al., 2013).

The $\delta^{18}O_{PO4}$ of silver phosphate produced from different rock samples, using different methods, are shown in Table 1. Most analyses were performed on silver phosphate prepared from whole rock powders using the ML-ON method, with duplicate preparations differing by $\leq \pm 0.25‰$. Close agreement was also found for the three whole rock samples prepared using both the ML-ON and the tooth enamel preparation methods (Table 1). For three rock samples there was no significant difference between the $\delta^{18}O$ values of silver phosphate prepared from apatite separates compared with whole rock powder; and only a 0.6‰ difference for a fourth sample. These comparisons in Table 1 give confidence in the use of the ML-ON method.

4.2. Primary magmatic carbonatites

$\delta^{18}O$ and $\delta^{13}C$ values for carbonate from Jacupiranga, Kaiserstuhl, Oka and Fen are between -4.5 to $-6.6‰$ $\delta^{13}C$ and $+7.6$ to $+8.2‰$ $\delta^{18}O$; values which are broadly within the PIC field of Jones et al. (2013) and similar to previous analyses from these carbonatites

(Table 1; Fig. 3). Apatite from these carbonatites, based on analysis of whole rocks and separates, has $\delta^{18}O_{PO4}$ values between $+4.1$ and $+5.4‰$. The St Honoré carbonatite has apatite $\delta^{18}O_{PO4}$ values and calcite $\delta^{13}C$ values within these same ranges, but the $\delta^{18}O$ value for calcite ($+16.4‰$) is significantly higher than the range for PIC.

4.3. Songwe carbonatite

One of the C1 carbonatites from Songwe had calcite $\delta^{13}C$ and $\delta^{18}O$ values within the PIC field (T0206, $\delta^{13}C = -3.4‰$, $\delta^{18}O = +7.8‰$). All other samples, however, trended towards much higher $\delta^{18}O$ values (up to $+26.7‰$) and, for some samples, slightly higher $\delta^{13}C$ values (Fig. 6).

The $\delta^{18}O_{PO4}$ values from Songwe range between $+3.0$ and $-0.7‰$ and are plotted in Fig. 7, arranged in approximate paragenetic order. All of the samples have $\delta^{18}O_{PO4}$ values lower than those for the primary magmatic carbonatites above. The highest $\delta^{18}O_{PO4}$ value at Songwe was found for apatite in the Mn-Fe vein. For all other samples there appears to be a trend for the $\delta^{18}O_{PO4}$ value to decrease as the carbonatite evolves.

5. Discussion

5.1. Towards a Primary Igneous Apatite field

If the post-magmatic isotope geochemistry of apatites is to be understood, we must first establish the probable range of $\delta^{18}O_{PO4}$ values for Primary Igneous Apatite (PIA). An estimate of the range of PIA $\delta^{18}O$ values can be made by applying an apatite-calcite fractionation to the accepted range of PIC $\delta^{18}O$ values. Fortier and Lüttge's (1995) experiments between 500 and 800 °C yielded a best fit fractionation of:

$$1000\ln\alpha_{ap-cc} = -0.68 - (1.60 \pm 0.26) \times 10^6 T^{-2} \qquad (1)$$

where $\alpha_{ap-cc} = (\delta^{18}O_{ap} + 1000)/(\delta^{18}O_{cc} + 1000)$

If we assume a formation temperature of 600–700 °C (the range established for the carbonatite solidus in a range of synthetic systems (Wyllie, 1966; Jago and Gittins, 1991)), then Eq. (1) yields $1000\ln\alpha_{ap-cc} = -2.78$ to -2.37. For a PIC $\delta^{18}O_{CC}$ range of $+5.3$ to $+8.4‰$ (Jones et al., 2013), the range for PIA $\delta^{18}O_{ap}$ is calculated to be $+2.5$ to $+6.0‰$.

Carbonatite samples from Oka, Jacupiranga, Tiksheozero, Siilinjärvi, Kaiserstuhl and Fen can all be texturally considered as primary carbonatites as they contain ovoid apatite forming at grain boundaries and/or in flow-banded clusters (Kapustin, 1980; Le Bas, 1989; Hogarth,
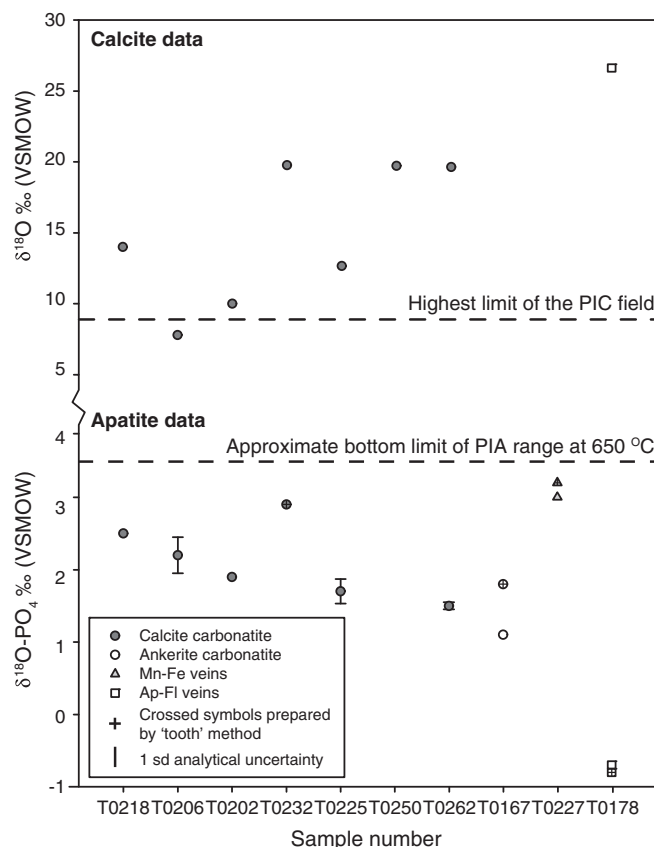

Fig. 7. Songwe $\delta^{18}O$ results from calcite (above) and $\delta^{18}O$ results from apatite (below), arranged in approximate paragenetic order. Error bars on apatite results represent replica values. Crossed symbols represent apatite results analysed by the 'tooth' method. Also included is the approximate bottom limit of the PIA and upper limit of the PIC field (Jones et al., 2013).

1989). Published values for apatite from Oka, Jacupiranga, Tiksheozero and Siilinjärvi (Conway and Taylor, 1969; Santos and Clayton, 1995; Tichomirowa et al., 2006; Fig. 2) all fall in the range $\delta^{18}O_{ap} = +4.2$ to $+5.7‰$ (n = 20), and our new analyses for Oka, Jacupiranga, Kaiserstuhl and Fen in the range $\delta^{18}O_{PO4} = +4.1$ to $+5.4‰$. These values are within the calculated PIA range, supporting the notion that it can be interpreted in a similar manner to the PIC field. Using more restricted ranges for the PIC field would accordingly narrow the PIA range. However, for this current dataset we believe it is better to keep a wider range of $+2.5$ to $+6.0‰$ until constrained by further data.

5.2. Is $\delta^{18}O_{PO4}$ susceptible to diffusion and isotopic resetting when interacting with a hydrothermal fluid?

Re-equilibration of minerals with subsequent fluids is a function of crystal geometry and structure, solution chemistry, pressure and temperature (Dodson, 1973; Cole and Chakraborty, 2001). While apatite readily exchanges O at higher temperatures, especially along the c-axis of the grain, it is relatively resistant to volume diffusion at lower temperatures compared to calcite (Farver and Giletti, 1989; Cole and Chakraborty, 2001). The apatite PO_4 site is, therefore, not likely to be susceptible to alteration from low-temperature fluids in carbonatites. A good example of this is apatite from the St Honoré carbonatite. Here, CL images show that the carbonatite has experienced at least two carbonate crystallisation stages, with early, euhedral, calcite (cal-1) overprinted by later anhedral carbonate(s) (cal-2) (Fig. 4). Apatite forms at grain-boundaries of cal-1, suggesting both minerals formed
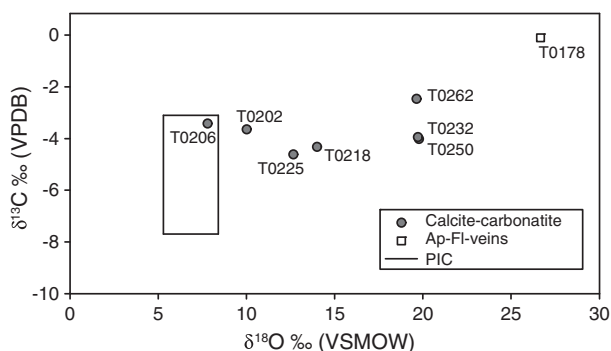

Fig. 6. $\delta^{18}O$ and $\delta^{13}C$ results for carbonates from Songwe, plotted against the PIC field (Jones et al., 2013).

in, or close to, equilibrium (Fig. 4). However, cal-2 forms along grain boundaries and within biotite cleavage planes, indicating later formation, out of equilibrium with apatite and the other major minerals in the sample. Oxygen isotope ratios from bulk carbonate analyses reach high values, up to 23‰ in the literature (Deines, 1989) and 16.4‰ in sample StH-2 (Fig. 3, Table 1). Such elevated $\delta^{18}O$ values are interpreted as representative of the later cal-2 stage recrystallising from interaction with low-temperature fluids which occur late in the carbonatite emplacement (Deines, 1989). Apatite from St Honoré, however, shows little textural evidence of interaction with cal-2 and the low-temperature fluid incursion. Its $\delta^{18}O_{PO_4}$ value falls into the PIA field, retaining the earlier, magmatic, record of the sample, while the $\delta^{18}O$ value from the carbonate records subsequent re-equilibration with lower temperature fluids. This is interpreted as evidence that apatite, once past its closure temperature, provides a good record of the isotopic conditions at crystallisation. Thus, any apatite which crystallised below 550 °C is likely to preserve the isotopic conditions of the crystallising fluid, rather than any subsequent fluid(s).

5.3. Using C and O isotopes to track the evolution of Songwe — carbonate data

Songwe carbonate $\delta^{18}O$ and $\delta^{13}C$ data show a broadly positive relationship ranging from T0206, in the PIC field, towards T0178, samples which are, respectively, early and late in the paragenesis of Songwe (Fig. 5). This is a common trend in carbonatites, and has been observed in carbonatites at Catalão (Santos and Clayton, 1995), Barro do Itapirapuã (Andrade et al., 1999), Ondurakorume, Kalkfeld, Dicker Willem, Spitskop (Horstmann and Verwoerd, 1997), Amba Dongar (Ray and Ramesh, 2006), Tamazeght (Marks et al., 2009), Lofdal (Do Cabo, 2014), Cummins Range (Downes et al., 2014) and Wicheeda (Trofanenko et al., 2016). These isotopic shifts could be caused by (Fig. 1): (1) sediment assimilation, (2) Rayleigh fractionation, or (3) low temperature alteration. A number of other processes, such as degassing, can still affect the final isotopic composition.

Sediment assimilation causes increased $\delta^{13}C$ due to incorporation of heavier carbon, from carbonate-bearing sediments, into water interacting with carbonatite. This process is unlikely to increase $\delta^{13}C$ in samples from Songwe as the country rock is a mixture of granulite and gneiss, with only very minor calc-silicate bands (up to a few cm) (Garson, 1965). None of these calc-silicate bands are found in immediate proximity to the carbonatite. Thus, the average carbon concentration in the country rock is low, and to cause large isotopic shifts through assimilation, the $\delta^{13}C$ ratio of the incorporated carbon will have to be very high. No carbon isotope data exist for marble bands from Malawi, but values from the continuation of the Mozambique Belt, in Mozambique, have ratios between −3.5 and −2.0‰ (Melezhik et al., 2008). Values of $\delta^{13}C$ from T0178 are higher and it seems highly unlikely that country rock assimilation could cause the increased carbonatite carbon isotope ratios.

Rayleigh fractionation of calcite from a fluid containing both CO_2 and H_2O leads to increased $\delta^{18}O$ and $\delta^{13}C$. Models for this process have been developed (Ray and Ramesh, 2000 and Santos and Clayton, 1995), and respective values for $\delta^{13}C$ and $\delta^{18}O$ for this process do not usually reach higher than −2‰ and 12‰, respectively (Ray and Ramesh, 2000). Thus, to reach the high $\delta^{18}O$ in the Songwe carbonatites, Rayleigh fractionation is, alone, an unlikely candidate. Furthermore, the general trend of $\delta^{18}O$ against $\delta^{13}C$ caused by Rayleigh fractionation in carbonatites is that of a positive correlation with a gradient of approximately 0.4 (Deines, 1989). This is a far higher gradient than observed in the Songwe stable isotope data (Fig. 6).

Low temperature alteration is capable of much larger changes in $\delta^{18}O$ than Rayleigh fractionation and has been suggested as the cause of high $\delta^{18}O$ in many carbonatites. The role of low-temperature alteration can be evaluated using models. Changes in C and O isotope ratios during low-temperature fluid-rock interaction between calcite, H_2O,

and CO_2 can be defined as a function of two mass-balance equations (Santos and Clayton, 1995; Ray and Ramesh, 1999):

$$\delta^{13}C_{rock}^{final} = \frac{\left(\frac{F_C}{R_C}\right)\left(\delta^{13}C_{fluid}^{initial} + \Delta_{rock-fluid}^C\right) + \delta^{13}C_{rock}^{initial}}{1 + \left(\frac{F_C}{R_C}\right)} \quad (2)$$

and:

$$\delta^{18}O_{rock}^{final} = \frac{\left(\frac{2r+2}{3r}\right)\left(\frac{F_C}{R_C}\right)\left(\delta^{18}O_{fluid}^{initial} + \Delta_{rock-fluid}^O\right) + \delta^{18}O_{rock}^{initial}}{1 + \left(\frac{2r+1}{3r}\right)\left(\frac{F_C}{R_C}\right)} \quad (3)$$

where:

F_C	moles of carbon in the fluid
R_C	moles of carbon in the rock
$\Delta^C_{rock-fluid}$	difference in carbon isotopes between the rock and the fluid
r	molar ratio of CO_2 to H_2O in the fluid

and:

$$\Delta_{rock-fluid}^O = 10^3 \ln\alpha^{18}O_{cc-CO_2} \\ + 10^3 \ln(1+2r) - 10^3 \ln(2r + \alpha^{18}O_{H_2O-CO_2}) \quad (4)$$

where $\alpha^{18}O_{cc-CO_2}$ and $\alpha^{18}O_{H_2O-CO_2}$ are fractionation factors between calcite–CO_2 and H_2O–CO_2, at a given temperature. Here, calcite is assumed to represent a bulk carbonatite rock. Fractionation factors for calcite–CO_2 are taken from Chacko et al. (1991), while H_2O–CO_2 is taken from Richet et al. (1977). Calculating $\Delta_{rock-fluid}^O$ using calcite-H_2O fractionation factors (following Santos and Clayton, 1995, and Demény and Harangi, 1996), from Friedman and O'Neil (1977), results in a similar model output (Supplementary Fig. 1).

These equations can be used to model the final isotopic composition of carbonate, under certain fluid conditions, in a closed system. They can only be used as a guide for interpretation as there are 6 unknowns: $\delta^{18}O_{rock}^{initial}$, $\delta^{13}C_{rock}^{initial}$, $\delta^{18}O_{fluid}^{initial}$, $\delta^{13}C_{fluid}^{initial}$, temperature, and r. Some of these unknowns can be reasonably assumed. Initial $\delta^{18}O$ and $\delta^{13}C$ is assumed to be from within the PIC field, while the fluid composition, if it is magmatically derived, would have a composition in equilibrium with the magma, but if it were meteoric, would have lower $\delta^{18}O$ values. Other assumptions cannot easily be made but the effects of different temperatures and CO_2/H_2O ratios can be incorporated onto different graphs and evaluated (see below).

Three models are presented in Fig. 8. The first two represent interaction of a PIC with deuteric fluid and meteoric fluid. Deep crustal fluids (e.g. metamorphic fluids) were discounted on the basis that the metamorphic country rock around Songwe is predominantly dry, with few hydrous mineral phases, and the shallow depth of intrusion at Songwe (Broom-Fendley et al., 2016c). The initial isotope values for the PIC ($\delta^{13}C_{rock}^{initial}$, $\delta^{18}O_{rock}^{initial}$) were chosen as $\delta^{18}O = +6$‰, $\delta^{13}C = -5$‰ because these values lie within the centre of the PIC field of Jones et al. (2013), and close to the values of T0206 which is texturally and isotopically the most primitive Songwe sample. For the deuteric fluid, the assumed isotopic composition was the same PIC values. The selected $\delta^{18}O$ value for meteoric fluid was −5‰, approximating meteoric water from a palaeo-latitude of around −45° (Bowen and Wilkinson, 2002; Bowen, 2010) which was the approximate position of Malawi at 130 Ma (Supplementary Fig. 2). A CO_2/H_2O ratio (r) of 0.001, representing a fluid with a low CO_2 activity, was selected following Santos and Clayton (1995). A higher ratio of 1000, representing a CO_2-rich fluid, has also been modelled in Fig. 8C for comparison. Intermediate values of r, representing mixed CO_2 and H_2O, cause steep changes in $\delta^{13}C$ and small changes in $\delta^{18}O$, leading to large $\delta^{13}C$ increases not observed in the data. For reference, these effects
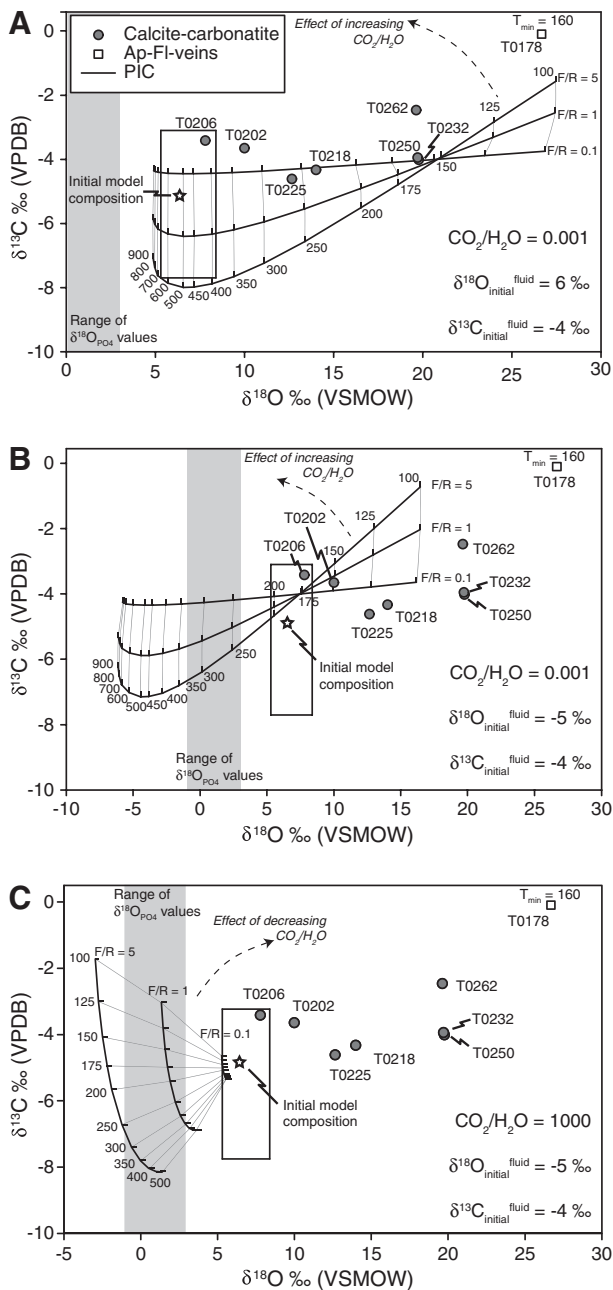
Fig. 8. Songwe stable isotope values compared with models for fluid-rock interaction between PIC and deuteric water (A), meteoric water (B), and CO_2-rich fluid (C) after Santos and Clayton (1995) and Ray and Ramesh (1999). Models are shown for fluid/rock ratios of 0.1, 1 and 5 (effectively ∞). Temperatures are shown in °C. The lowest 'cut-off' temperature of 160 °C from fluid inclusion homogenisation temperatures in fluorite is indicated for sample T0178.

are sketched onto Fig. 8. The isotopic ratios are modelled between 900 and 100 °C, spanning the most-likely temperature range of the system with the lower limit constrained by a minimum temperature of 160 °C from fluid-inclusion data (Broom-Fendley et al., 2016b). Three different fluid/rock ratios (F_C/R_C) have been included in Fig. 8: 0.1, 1 and 5, representing minor, moderate and complete alteration, respectively.

The models indicate that when deuteric water starts to cool below 400 °C, the $\delta^{18}O$ values of the rock increase from the PIC field. For low degrees of alteration (i.e. low F/R ratios), this is accompanied by negligible $\delta^{13}C$ change, while at higher degrees of alteration modest changes (up to approximately −2‰) in $\delta^{13}C$ occur (Fig. 8A). Meteoric fluid alteration above 200 °C leads to lower $\delta^{18}O$ than PIC for all degrees of

alteration. At temperatures below 175 °C, $\delta^{18}O$ increases to values higher than the PIC field, accompanied by little $\delta^{13}C$ change at low degrees of alteration, but higher $\delta^{13}C$ with complete alteration (Fig. 8B). A CO_2-rich fluid, conversely, results in lower $\delta^{18}O$ values of the rock, accompanied by decreasing $\delta^{13}C$ above 200 °C and increasing $\delta^{13}C$ at lower temperatures. Increasing degrees of alteration lead to lower $\delta^{18}O$ values and more extreme variation in $\delta^{13}C$ (Fig. 8C).

Based on the above models, it is clear that low temperature alteration, from either deuteric or meteoric water, can cause large increases in $\delta^{18}O$, while alteration from a CO_2-rich fluid leads to moderately lower $\delta^{18}O$ values (Deines, 1989; Santos and Clayton, 1995; Ray and Ramesh, 1999; Fig. 8). It is clear that the model for a CO_2-rich fluid does not best represent the carbonate data, suggesting these values are caused by alteration from a CO_2-poor fluid of meteoric or deuteric origin. Deuteric alteration at high temperatures causes minimal changes to the isotopic ratios of the final carbonate while meteoric water at high temperature can shift $\delta^{18}O$ to lower values. It is important to note, however, that these closed-system models represent only the extreme of what can occur in carbonatites (i.e. 100% meteoric water or 100% deuteric water). Furthermore, they do not represent open-system processes, although these can be qualitatively assessed from interpretation of the model output (see Section 5.5).

Low-temperature alteration also increases $\delta^{13}C$ towards lower temperatures. This is a function of increasing carbon isotope fractionation between the carbon in the fluid (assumed to be a dissolved species) and the precipitating carbonate mineral. At lower temperatures, and at higher C concentration in the fluid, the effect of this fractionation is greater and thus the $\delta^{13}C$ value of the final product is higher than the initial model composition (−4‰ for both meteoric and deuteric water). Carbonate stable isotope data from Songwe broadly plot along the line of alteration from a deuteric fluid at decreasing temperature (Fig. 8A), although it should be noted that above 200 °C, the O isotope fractionation between calcite and CO_2 is negative and the isotopic composition of crystallising calcite would be below that of the modelled fluid (Chacko et al., 1991).

5.4. Using O isotopes to track the evolution of Songwe — apatite data

The results for $\delta^{18}O_{PO4}$ in Fig. 7 are plotted in paragenetic order. This is perhaps a subjective order in which to present the data, and samples T0202–T0262 could be rearranged depending on re-interpretation of the other minerals in the sample. Nevertheless, samples T0218, T0167 and T0178 are paragenetically well constrained as they all contain apatite which clearly belongs to a particular type: T0218 contains Ap-1 and Ap-2 from early magmatic calcite carbonatite; T0167, contains Ap-3 from Fe-rich carbonatite; and in T0178 the apatite is Ap-4, from Chenga Hill, outside the Songwe carbonatite (Broom-Fendley et al., 2016b). Apatite in T0206 is also predominantly Ap-1/2, similar to T0218, but the sample also contains a small percentage of Ap-3. Samples T0202–T0262 are all Ap-3 -bearing samples from calcite carbonatite. Thus, although T0202–T0262 can be rearranged, the samples in Fig. 7 are still in the order of Ap-1, 2, 3, 4.

Excluding sample T0227, samples which have crystallised from more evolved fluids at Songwe show lower $\delta^{18}O_{PO4}$ values, in contrast to increasing carbonate $\delta^{18}O$ (Fig. 7), and are lower than the PIA values. Few mechanisms reduce the $\delta^{18}O$ value of a mineral crystallising in a carbonatite. It is rarely documented, and has only been observed in rocks at the Igaliko dyke swarm (syn. Igaliku), Gardar Province, Greenland (Pearce and Leng, 1996); in rødberg (calcite or calcite–dolomite carbonite with hematite alteration) from Fen, Norway (Andersen, 1984); and in the Arshan carbonatite, Transbaikalia, Russia (Doroshkevich et al., 2008).

At Igaliko, high fluorine (F) contents are carried by fluids with lower $\delta^{18}O$ values, and the F content could be the cause of $\delta^{18}O$ suppression (Pearce and Leng, 1996; Pearce et al., 1997). At Fen, post-magmatic hydrothermal oxidation by meteoric water is proposed as the mechanism

for lowering the $\delta^{18}O$ of ferrocarbonatite, forming rødberg (haematite-carbonatite; Andersen, 1984). In rødberg, $\delta^{18}O$ is lower than ferrocarbonatite by 2‰ and formed at an estimated temperature of 250–300 °C. This reduction in $\delta^{18}O$ is calculated to have been caused by a fluid with a $\delta^{18}O$ value lower than 0.8‰; a composition reconcilable with meteoric water, but not deuteric water (Andersen, 1984). At Arshan, calcite is texturally recrystallised, this is reflected in its $\delta^{18}O$ values which lie between −4‰ and −7.2‰. Isotope data from altered bastnäsite-(Ce), allanite-(Ce) and phlogopite form a continuum between the PIC field and the calcite data and Doroshkevich et al. (2008) estimate that the composition of an altering fluid would have been between −10 to −15‰ at a temperature of 345–397 °C. These compositions correspond to meteoric water values.

High concentrations of F in the mineralising fluid at Songwe cannot be ruled out and if high F concentrations have a strong effect on $\delta^{18}O$, then the role of fluorine cannot entirely be discounted. However, recent experimental work on the solubility of REE fluoride minerals (Migdisov and Williams-Jones, 2014), and the low F contents in REE mineralised rocks from Kangankunde (Wall, 2000), suggests a less significant role for F in the process of hydrothermal REE transport than has previously been considered. It is unlikely that a change in the apatite O-isotope ratio was caused by low-temperature exchange with groundwater, post-emplacement, as apatite is not susceptible to low temperature dissolution-reprecipitation.

To aid in the interpretation of the apatite isotope data, the models derived for isotopic variations in carbonates can be used as a guide (Fig. 8). These models indicate that one way of achieving carbonate with $\delta^{18}O$ values lower than primary carbonatite is through invoking a meteoric water component (modelled as $\delta^{18}O = -5$‰) at a temperature above 200 °C. Meteoric water with a lower initial $\delta^{18}O$ value will reduce the $\delta^{18}O$ of the carbonate at lower temperatures. These principles can be used to help understand the $\delta^{18}O_{PO4}$ data. Values for $\delta^{18}O_{PO4}$ decrease later in the paragenetic sequence but, if the composition of the fluid remains the same during this sequence, the only explanation would be increasing fluid temperature. This is not plausible and a more likely interpretation is that decreasing $\delta^{18}O_{PO4}$ is due to an increasing proportion of meteoric water in the fluid towards the late stages of crystallisation. This requires open-system evolution of carbonatites, incorporating more meteoric water as they cool.

An alternative cause for the lower $\delta^{18}O$ values in the apatite could be through interaction with CO_2-rich fluids, rather than H_2O-rich fluids. Fractionation between calcite and CO_2 is negative and decreases between 500 and 100 °C, with values for $10^3 \ln\alpha_{cc-CO2}$ between −6 and −12‰ (Chacko et al., 1991; Chacko and Deines, 2008). Thus, assuming fractionation between apatite and CO_2 is similar to calcite and CO_2, apatite crystallising from a cooling CO_2-rich fluid will have progressively lower $\delta^{18}O$ values (Santos and Clayton, 1995). Interaction with CO_2-rich fluids (i.e., those with a high CO_2/H_2O ratio, e.g. 1000) can be modelled similarly to H_2O-rich fluids, as indicated on Fig. 8C. Comparison of the apatite data-range with these models indicates that, in addition to a meteoric water input, increasing degrees of fluid-rock interaction with a cooling CO_2-rich fluid could cause the $\delta^{18}O$ values observed in the apatite data.

5.5. Reconciling calcite $\delta^{18}O$ and apatite $\delta^{18}O_{PO4}$ data

Diverging trends for $\delta^{18}O_{PO4}$ in apatite and $\delta^{18}O$ in calcite cannot be accounted through equilibrium fractionation between the two minerals at different temperatures. Even if fractionation occurs at 0 °C, the fractionation factor between apatite and calcite is below 10‰. Fractionation at higher temperatures results in a smaller fractionation factor (Fortier and Lüttge, 1995). Thus, offsets in $\delta^{18}O$ of approximately 25‰ between calcite and apatite, as is observed in T0178, cannot be produced by equilibrium fractionation and, thus, the two minerals are not in equilibrium. This is further supported by the ambiguous textural relationship

between apatite and calcite, where calcite appears to form both before, during, and after apatite crystallisation (Fig. 5).

One way to reconcile the diverging apatite and calcite data is through an open-system, meteoric mixing model which effectively combines the models of Fig. 8A and B. In such a model, an initial deuteric fluid, with C and O isotope ratios in equilibrium with carbonatite, gradually mixes with meteoric water as temperature drops. Isotopic variation in the apatite requires cooling of a fluid from a high temperature and further incorporation of meteoric water, while for calcite, the model requires the same, but at cooler temperatures. It is difficult to quantitatively reconcile these divergent trends but it is possible to show, conceptually, that a cooling fluid, incorporating an increasing proportion of meteoric water can first, at high temperatures, shift the isotopic composition of the products to lower $\delta^{18}O$ isotope values, before, at lower temperature, trending towards higher $\delta^{18}O$ (Fig. 9A). Such a model is based on many assumptions and should only be used as a rough guide. The most critical assumption, for which few constraining factors are available, is the rate at which meteoric water and deuteric water mix, and the relationship of this with temperature. A linear relationship between temperature and meteoric water concentration has been selected for simplicity:

$$\%_{Meteoric\,water} = -0.2T + 100 \qquad (5)$$

While it is logical to assume that over time, and thus with decreasing temperature, the percentage of meteoric water in a carbonatite system will increase, there is no geological justification for a linear relationship
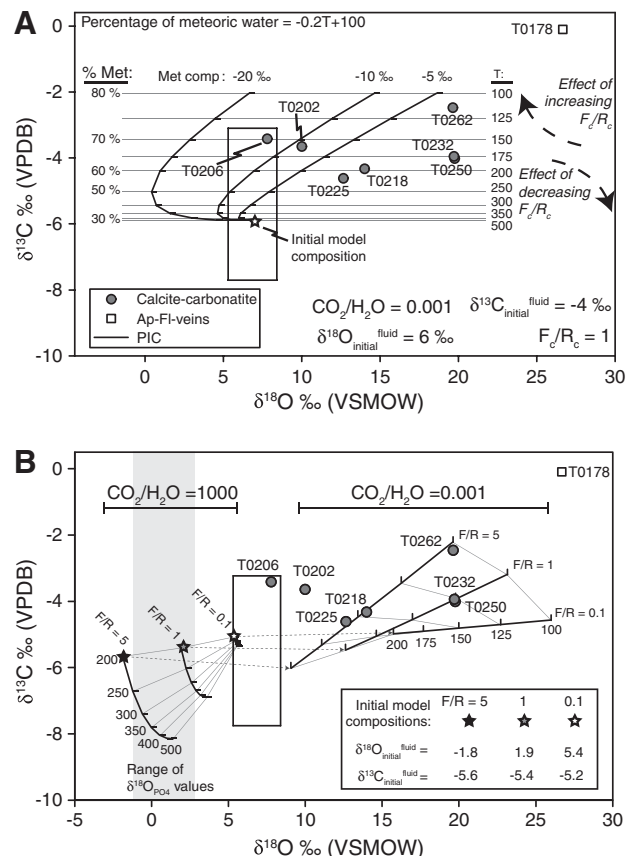

Fig. 9. Conceptual models to reconcile the apatite and calcite data. (A) Mixing between meteoric water and deuteric water, based on fluid-alteration models after Santos and Clayton (1995) and Ray and Ramesh (1999), but incorporating a linear relationship between the temperature and composition of the fluids, such that $\%_{Meteoric\,Fluid} = -0.2\,T + 100$. (B) Depressurisation of a CO_2-rich fluid based on a hybrid of models in Fig. 8A and C. A rapid change from CO_2-rich (r = 1000) to H_2O-rich (r = 0.001) fluids, is modelled at 200 °C, resulting in significant change in the $\delta^{18}O$ values.

between these two factors. Perhaps more likely, given the high degree of brecciation at Songwe Hill, is that of a sudden influx of meteoric water, and a rapid decrease in temperature — akin to a depressurisation event (Broom-Fendley et al., 2016c). This is, however, difficult to model as it requires a judgement of when (at what temperature) to place the influx of meteoric water. Therefore, a simple linear relationship has been retained until this can be better constrained. Other assumptions in the model include treating the composition of the fluid (r) and the fluid/rock ratio (F_c/R_c) as constant. Of course, if meteoric water was mixing with magmatic water, the CO_2 concentration in the water would decrease and the degree of alteration would progressively increase. Both of these variables were kept constant in the conceptual model to show only the effects of temperature and isotopic composition. Despite the assumptions made in the models, they clearly show a common trend when mixing meteoric and deuteric water. First, $\delta^{18}O$ values decrease before, at lower temperatures, extending to higher values. This trend suggests that open-system mixing between meteoric and deuteric water may cause the observed divergent isotope data in the different minerals.

An alternative to a deuteric-meteoric mixing model could be a change in fluid composition: from CO_2-rich to H_2O-rich. A CO_2-rich fluid is capable of lowering apatite $\delta^{18}O$ values from the PIC field as it cools (Fig. 8C). A depressurisation event, as previously mentioned, could also cause rapid degassing of a carbonatite fluid, corresponding with a sudden decrease in the CO_2/H_2O ratio. Such a sudden change in the CO_2/H_2O ratio would mean that the role of CO_2 in the fluid becomes negligible and that H_2O causes later changes in $\delta^{18}O$ at lower temperatures. This would result in subsequently crystallising minerals having higher $\delta^{18}O$ values, as modelled for carbonates in Fig. 8A. Similarly to the deuteric-meteoric fluid mixing, it is possibly to conceptually model the process of degassing by combining the models demonstrated in Fig. 8A and C (Fig. 9B). In the illustrated model, degassing is assumed to occur at 200 °C although a similar trend would occur over a much wider temperature range. This degassing is conceptually modelled as an instantaneous change from a CO_2-rich fluid to a H_2O-rich fluid, with r changing from 1000 to 0.001. The conditions for the CO_2-rich fluid are the same as in Fig. 8C, but the conditions for the H_2O vary based on the final fluid composition of the CO_2-rich fluid. These models illustrate that a sudden change from a CO_2-rich to a H_2O-rich fluid could account for the range of $\delta^{18}O$ values observed in the apatite and carbonate data. Apatite, crystallising earlier than calcite, records a 'CO_2-rich signal' while recrystallisation of subsequent carbonates records a 'H_2O-rich signal'. These models, however, illustrate a single stage process and it is highly likely that multiple stages of fluid influx could occur. Late influx of meteoric water could account for the extremely elevated $\delta^{18}O$ values in sample T0178.

5.6. Compositional estimates for mineralising water

Combining the isotope data with homogenisation temperatures from fluid inclusions enables calculation of the composition of water crystallising HREE-enriched apatite. Sufficiently reliable homogenisation temperatures in apatite were obtained from samples from Fe-rich carbonatite (T0167, 200 °C) and from apatite-fluorite veins from Chenga (T0178, 160 °C; Broom-Fendley et al., 2016b). The isotopic composition of water in equilibrium with apatite at these temperatures, calculated using the apatite-water data from Zheng (1996), is $\delta^{18}O_{H2O} = -4.0‰$ for T0167 and $-7.8‰$ for T0178. These values further suggest an increased role for meteoric water later in the paragenetic sequence.

5.7. A model for the mineralising fluid

Using the new isotope data, a model for the transport and deposition of the HREE is proposed (Fig. 10). A PIA value for Songwe is likely to be between 4 and 6‰ for O, using the PIA data from the other carbonatites.

Apatite in this stage is LREE-enriched, typical of magmatic apatite (Broom-Fendley et al., 2016b).

Ap-2 represents the first stages of HREE enrichment at Songwe. It is difficult to estimate the isotopic composition of the fluid which Ap-2 formed from as Ap-2 is mixed with Ap-1. If Ap-1 is between 4 and 6‰, then Ap-2 must have $\delta^{18}O_{PO4}$ values lower than 2.5‰ to balance the proportion of Ap-1 with lower $\delta^{18}O_{PO4}$ in these samples. This cannot be resolved with the current dataset and requires spatially-resolved stable isotope data. Nevertheless, the combined values of Ap-1 and Ap-2 are clearly lower than might be expected from PIA. These values are interpreted as influenced by a cooling CO_2-rich fluid or an indication of the first effects of an influx of meteoric water.

Ap-1 and Ap-2 are only found in clasts of C1 calcite carbonatite, indicating that brecciation took place after the formation of these apatite types (Broom-Fendley et al., 2016c). Brecciation could have been caused by depressurisation of CO_2 from a dissolved fluid, or overpressure of a fluid trapped in the carbonatite. After brecciation, calcite carbonatite (C2) containing Ap-3 is widespread. In a few samples, it can be found in association with Ap-1 and 2, but typically it forms large anhedral masses interpreted to be formed in a hydrothermal environment. The HREE-bearing fluid was initially likely to be predominantly CO_2-rich, with an O isotope ratio between 0 and 5‰. This fluid transported the REE, preferentially carrying the LREE, away from the carbonatite (cf. Downes et al., 2014; Cooper et al., 2015; Broom-Fendley et al., 2016a). Depressurisation would cause the fluid to become rapidly H_2O-rich, and the low solubility of apatite would cause it to crystallise early, at a relatively high temperature (Broom-Fendley et al., 2016b), retaining the low $\delta^{18}O$ values of the fluid. After brecciation it would be easier for meteoric fluids to interact with the carbonatite, and it is suggested that a convection cell was established soon after brecciation occurred (Fig. 10). Such a convection cell could be driven by the cooling of the neighbouring Mauze nepheline syenite (Broom-Fendley et al., 2016c). As the convection cell becomes increasingly diluted with meteoric water, the salinity, temperature and O-isotope ratio of the fluid decreases. These changes cause other LREE minerals to crystallise later in the paragenetic sequence. In areas where the Ca concentration is low, such as outside the main carbonatite, there is insufficient Ca to form apatite, and thus xenotime forms instead (e.g. T0178).

As the system cools, dissolution-reprecipitation of calcite continues to lower temperatures, causing the O-isotope ratios in the calcite to increase to values up to 27‰. At these lower temperatures, however, the fluid does not affect the isotopic composition of the already-crystallised apatite, and the high-T low $\delta^{18}O$ values are preserved.

6. Conclusions

A new method for analysing oxygen isotopes in apatite has been presented. This method has been used, in combination with conventional O and C isotope analyses of carbonates, to measure the isotopic ratios of apatite and carbonate from several different carbonatites with magmatic textures.

The new method of determining O isotope ratios in apatite is a bulk-rock technique where oxygen is analysed from the more stable apatite PO_4 site. To check the validity of this new bulk-powder technique, five carbonatite samples were prepared as hand-picked apatite separates and analysed in the same way as the bulk powder samples. The results showed no significant difference, falling within 2σ analytical uncertainty.

When interpreting O isotope data from carbonatites it is common to evaluate the data relative to a PIC range. Since no data exists for the apatite PO_4 site from PIC, a range for PIA has been calculated and tested by analysing the PO_4 site of four apatite samples from globally distributed carbonatites which display primary crystallisation textures. The preliminary range determined for PIA is 2.5 to 6.0‰.

Ten samples from the Songwe Hill carbonatite were analysed, with 9 apatite and 8 carbonate analyses carried out in total. Carbonate C and O
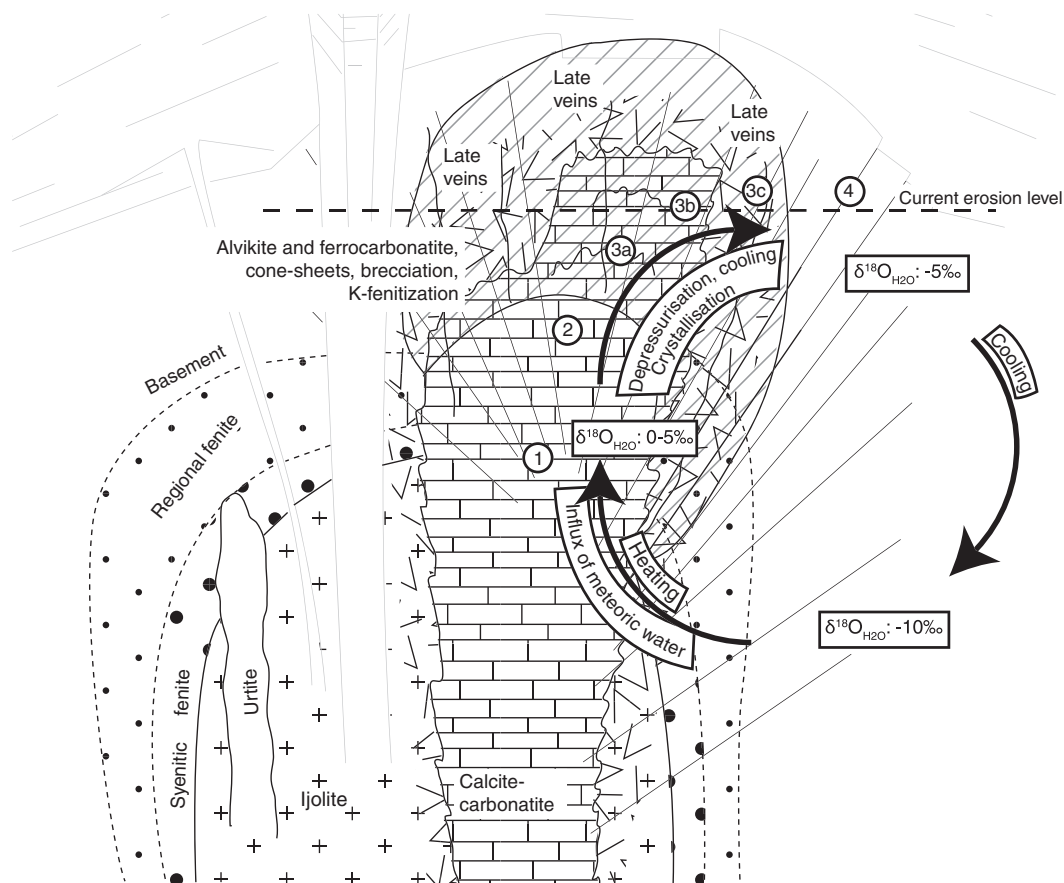
Fig. 10. A schematic model for fluid transport around a carbonatite based on the carbonatite model after Le Bas (1987). A CO_2-rich fluid (1), with an initial $\delta^{18}O$ value of approximately 0–5‰, carries the HREE (2). Depressurisation leads to rapid CO_2 loss and HREE-rich apatite crystallisation (3a, 3b). Subsequently, an influx of meteoric water occurs, with a lower salinity, temperature and $\delta^{18}O$ value. As the solutions mix, the REE-bearing deuteric fluid is diluted, the isotopic ratio of the water decreases and the temperature drops. This causes LREE fluorcarbonates to precipitate out of solution (3c). The cycle continues and, as the fluid cools, it re-circulates into the carbonatite, causing further dissolution and re-precipitation of calcite (4), causing the calcite $\delta^{18}O$ values to increase. Apatite, however, is unaffected by this low temperature fluid and records the isotopic conditions under which the HREE were originally precipitated. Numbers also refer to Fig. 5.

isotope results show a general trend, from early to late in the paragenetic sequence, towards higher $\delta^{18}O$ values, with a slight increase in $\delta^{13}C$. Oxygen isotope ratios from apatite show a contrary trend, with values decreasing from the PIA field towards more negative values. The large increases in $\delta^{18}O$ in the carbonate results are interpreted as the result of low temperature fluid interaction, derived from either a meteoric or deuteric source. Modelling shows that both fluid sources are possible and it is suggested that the changes in calcite stable isotope ratios are caused by a contribution from each reservoir. The decreases in $\delta^{18}O_{PO4}$ in the apatite are interpreted as a preserved record of earlier interaction with a CO_2-rich deuteric fluid, or from an early influx of hot meteoric water. This interaction has been preserved due to the lower susceptibility of apatite, relative to calcite, to alteration from low temperature fluids. The diverging trends are conceptually reconciled with simple mixing models between deuteric, meteoric water, and CO_2-rich fluids.

Based on the isotope data, a model is proposed where HREE mineralisation occurs rapidly after brecciation and depressurisation. Subsequently, a convection cell develops, interacting with the surrounding meteoric water. It is proposed that the LREE are transported in the fluids of this convection cell and precipitate through further mixing with meteoric water, due to decreasing salinity and/or temperature.

Appendix A. Supplementary data

Supplementary data to this article can be found online at http://dx.doi.org/10.1016/j.chemgeo.2016.07.023.

References

Andersen, T., 1984. Secondary processes in carbonatites: petrology of 'Rødberg' (hematite-calcite-dolomite carbonatite) in the Fen central complex, Telemark (South Norway). Lithos 17, 227–245.

Andersen, T., 1987. Mantle and crustal components in a carbonatite complex, and the evolution of carbonatite magma: REE and isotopic evidence from the Fen complex, southeast Norway. Chem. Geol. 65, 147–166.

Andrade, F., Möller, P., Lüders, V., Dulski, P., Gilg, H., 1999. Hydrothermal rare earth elements mineralization in the Barra do Itapirapuã carbonatite, southern Brazil: behaviour of selected trace elements and stable isotopes (C, O). Chem. Geol. 155, 91–113.

Barth, T., Ramberg, I., 1966. The Fen circular complex. In: Tuttle, O., Gittins, J. (Eds.), Carbonatites. Interscience, New York, p. 257.

Bowen, G.J., 2010. Isoscapes: spatial patterns in isotopic biogeochemistry. Annu. Rev. Earth Planet. Sci. 38, 161–187.

Bowen, G.J., Wilkinson, B., 2002. Spatial distribution of $\delta^{18}O$ in meteoric precipitation. Geology 30, 315–318.

Broom-Fendley, S., Styles, M.T., Appleton, J.D., Gunn, G., Wall, F., 2016a. Evidence for dissolution-reprecipitation of apatite and preferential LREE mobility in carbonatite-derived late-stage hydrothermal processes. Am. Mineral. 101, 596–611.

Broom-Fendley, S., Brady, A.E., Wall, F., Gunn, G., Dawes, W., 2016b. REE minerals at the Songwe Hill carbonatite, Malawi: HREE-enrichment in late-stage apatite. Ore Geol. Rev. in revision.

Broom-Fendley, S., Brady, A.E., Horstwood, M.S.A., Mtegha, J., Woolley, A., Wall, F., Dawes, W., Gunn, G., 2016c. Geology, Geochemistry and Geochronology of the Songwe Hill Carbonatite and Mauze Nepheline Syenite Complex, Malawi: Some Implications for the Genesis of the Chilwa Alkaline Province submitted for publication.

Burmann, F., Keim, M.F., Oelmann, Y., Teiber, H., Marks, M.A., Markl, G., 2013. The source of phosphate in the oxidation zone of ore deposits: evidence from oxygen isotope compositions of pyromorphite. Geochim. Cosmochim. Acta 123, 427–439.

Chacko, T., Deines, P., 2008. Theoretical calculation of oxygen isotope fractionation factors in carbonate systems. Geochim. Cosmochim. Acta 72, 3642–3660.

Chacko, T., Mayeda, T.K., Clayton, R.N., Goldsmith, J.R., 1991. Oxygen and carbon isotope fractionations between CO_2 and calcite. Geochim. Cosmochim. Acta 55, 2867–2882.

Chakhmouradian, A.R., Reguir, E.P., Zaitsev, A.N., 2016. Calcite and dolomite in intrusive carbonatites. I. Textural variations. Mineral. Petrol. 110, 333–360.

Chenery, C.A., Pashley, V., Lamb, A.L., Sloane, H.J., Evanse, J.A., 2012. The oxygen isotope relationship between the phosphate and structural carbonate fractions of human bioapatite. Rapid Commun. Mass Spectrom. 26, 309–319.

Cole, D.R., Chakraborty, S., 2001. Rates and mechanisms of isotopic exchange. Rev. Mineral. Geochem. 43, 83–223.

Conway, C.M., Taylor, H.P., 1969. O^{18}/O^{16} and C^{13}/C^{12} ratios of coexisting minerals in the Oka and Magnet Cove carbonatite bodies. J. Geol. 77, 618–626.

Cooper, A.F., Collins, A.K., Palin, J.M., Spratt, J., 2015. Mineralogical evolution and REE mobility during crystallisation of ancylite-bearing ferrocarbonatite, Haast River, New Zealand. Lithos 216–217, 324–337.

Costanzo, A., Moore, K.R., Wall, F., Feely, M., 2006. Fluid inclusions in apatite from Jacupiranga calcite carbonatites: evidence for a fluid-stratified carbonatite magma chamber. Lithos 91, 208–228.

Croll, R., Swinden, S., Hall, M., Brown, C., Beer, G., Scheepers, J., Redellinghuys, T., Wild, G., Trusler, G., 2014. Mkango Resources Limited., Songwe REE project, Malawi: NI 43-101 pre-feasibility report. Technical Report. MSA Group (Pty) Ltd.

Dean, J.R., Jones, M.D., Leng, M.J., Noble, S.R., Metcalfe, S.E., Sloane, H.J., Sahy, D., Eastwood, W.J., Roberts, N., 2015. Eastern Mediterranean hydroclimate over the late glacial and Holocene, reconstructed from the sediments of Nar lake, central Turkey, using stable isotopes and carbonate mineralogy. Quat. Sci. Rev. 124, 162–174.

Deines, P., 1970. The carbon and oxygen isotopic composition of carbonates from the Oka carbonatite complex, Quebec, Canada. Geochim. Cosmochim. Acta 34, 1199–1225.

Deines, P., 1989. Stable isotope variations in carbonatite. In: Bell, K. (Ed.), Carbonatites: Genesis and Evolution. Unwin Hyman, London.

Deines, P., Gold, D., 1973. The isotopic composition of carbonatite and kimberlite carbonates and their bearing on the isotopic composition of deep-seated carbon. Geochim. Cosmochim. Acta 37, 1709–1733.

Demény, A., Harangi, S., 1996. Stable isotope studies and processes of carbonate formation in Hungarian alkali basalts and lamprophyres: evolution of magrnatic fluids and magma-sediment interactions. Lithos 37, 335–349.

Demény, A., Fórizs, I., Molnár, F., 1994. Stable isotope and chemical compositions of carbonate ocelli and veins in Mesozoic lamprophyres of Hungary. Eur. J. Mineral. 6, 679–690.

Demény, A., Ahijado, A., Casillas, R., Vennemann, T., 1998. Crustal contamination and fluid/rock interaction in the carbonatites of Fuerteventura (Canary Islands, Spain): a C, O, H isotope study. Lithos 44, 101–115.

Demény, A., Vennemann, T., Ahijado, A., Casillas, R., 2004a. Oxygen isotope thermometry in carbonatites, Fuerteventura, Canary Island, Spain. Mineral. Petrol. 80, 155–172.

Demény, A., Sitnikova, M., Karchevsky, P., 2004b. Stable C and O isotope compositions of carbonatite complexes of the Kola Alkaline Province: phoscorite-carbonatite relationships and source compositions. In: Wall, F., Zaitsev, A. (Eds.), Phoscorites and Carbonatites from Mantle to Mine: The Key Example of the Kola Alkaline Province. Mineralogical Society Series vol. 10, p. 407.

Do Cabo, V., 2014. Geological, Geochemical and Mineralogical Characteristics of the HREE-Rich Carbonatites at Lofdal, Namibia PhD thesis University of Exeter.

Dodson, M.H., 1973. Closure temperature in cooling geochronological and petrological systems. Contrib. Mineral. Petrol. 40, 259–274.

Doroshkevich, A.G., Ripp, G.S., Viladkar, S.G., Vladykin, N.V., 2008. The Arshan REE carbonatites, southwestern Transbaikalia, Russia: mineralogy, paragenesis and evolution. Can. Mineral. 46, 807–823.

Downes, P.J., Demény, A., Czuppon, G., Jaques, A.L., Verrall, M., Sweetapple, M., Adams, D., McNaughton, N.J., Gwalani, L.G., Griffin, B.J., 2014. Stable H–C–O isotope and trace element geochemistry of the Cummins Range Carbonatite Complex, Kimberley region, Western Australia: implications for hydrothermal REE mineralization, carbonatite evolution and mantle source regions. Mineral. Deposita 49, 905–932.

Farquhar, J., Chacko, T., Frost, B.R., 1993. Strategies for high temperature oxygen isotope thermometry: a worked example from the Laramie Anorthosite Complex, Wyoming, USA. Earth Planet. Sci. Lett. 117, 407–422.

Farver, J.R., Giletti, B.J., 1989. Oxygen and strontium diffusion kinetics in apatite and potential applications to thermal history determinations. Geochim. Cosmochim. Acta 53, 1621–1631.

Fortier, S.M., Lüttge, A., 1995. An experimental calibration of the temperature dependence of oxygen isotope fractionation between apatite and calcite at high temperatures (350–800 °C). Chem. Geol. 125, 281–290.

Friedman, I., O'Neil, J.R., 1977. Compilation of stable isotope fractionation factors of geochemical interest. Data of Geochemistry. U.S. Geol. Survey., Professional. Paper., 440-KK, sixth ed.

Garson, M., 1965. Carbonatites in southern Malawi. Bull. Geol. Surv. Malawi 15.

Garvie-Lok, S.J., Varney, T.L., Katzenberg, M.A., 2004. Preparation of bone carbonate for stable isotope analysis: the effects of treatment time and acid concentration. J. Archaeol. Sci. 31, 763–776.

Gold, D.P., Eby, G.N., Bell, K., Vallée, M., 1986. Carbonatites, diatremes and ultra-alkaline rocks in the Oka area, Quebec. Guidebook: Fieldtrip 21. Geological Association of Canada-Mineralogical Association of Canada-Canadian Geophysical Union, Ottawa 51 pp.

Greenwood, J.P., Blake, R.E., Coath, C.D., 2003. Ion microprobe measurements of $^{18}O/^{16}O$ ratios of phosphate minerals in the martian meteorites ALH84001 and Los Angeles. Geochim. Cosmochim. Acta 67, 2289–2298.

Grimes, S.T., Collinson, M.E., Hooker, J.J., Mattey, D.P., 2008. Is small beautiful? A review of the advantages and limitations of using small mammal teeth and the direct laser fluorination analysis technique in the isotope reconstruction of past continental climate change. Palaeogeogr. Palaeoclimatol. Palaeoecol. 266, 39–50.

Haynes, E.A., Moecher, D.P., Spicuzza, M.J., 2003. Oxygen isotope composition of carbonates, silicates, and oxides in selected carbonatites: constraints on crystallization temperatures of carbonatite magmas. Chem. Geol. 193, 43–57.

Hoefs, J., 2008. Stable Isotope Geochemistry. Springer.

Hogarth, D., 1989. Pyrochlore, apatite and amphibole: distinctive minerals in carbonatite. In: Bell, K. (Ed.), Carbonatites: Genesis and Evolution. Unwin Hyman, London.

Horstmann, U.E., Verwoerd, W.J., 1997. Carbon and oxygen isotope variations in southern African carbonatites. J. Afr. Earth Sci. 25, 115–136.

Hubberten, H.-W., Katz-Lehnert, K., Keller, J., 1988. Carbon and oxygen isotope investigations in carbonatites and related rocks from the Kaiserstuhl, Germany. Chem. Geol. 70, 257–274.

Jago, B.C., Gittins, J., 1991. The role of fluorine in carbonatite magma evolution. Nature 349, 56–58.

Jones, A.P., Genge, M., Carmody, L., 2013. Carbonate melts and carbonatites. Rev. Mineral. Geochem. 75, 289–322.

Kapustin, I., 1980. Mineralogy of Carbonatites. Amerind Publishing Co., New Dehli.

Keller, J., 1981. Carbonatitic volcanism in the Kaiserstuhl alkaline complex: evidence for highly fluid carbonatitic melts at the Earth's surface. J. Volcanol. Geotherm. Res. 9, 423–431.

Keller, J., Hoefs, J., 1995. Stable isotope characteristics of recent natrocarbonatites from Oldoinyo Lengai. In: Bell, K., Keller, J. (Eds.), Carbonatite Volcanism. Springer, pp. 113–123.

Koch, P.L., Tuross, N., Fogel, M.L., 1997. The effects of sample treatment and diagenesis on the isotopic integrity of carbonate in biogenic hydroxylapatite. J. Archaeol. Sci. 24, 417–429.

Kohn, M.J., Cerling, T.E., 2002. Stable isotope compositions of biological apatite. Rev. Mineral. Geochem. 48, 455–488.

Kolodny, Y., Luz, B., Navon, O., 1983. Oxygen isotope variations in phosphate of biogenic apatites, I. Fish bone apatite—rechecking the rules of the game. Earth Planet. Sci. Lett. 64, 398–404.

Le Bas, M., 1987. Nephelinites and carbonatites. Geol. Soc. Lond., Spec. Publ. 30, 53–83.

Le Bas, M., 1989. Diversification of carbonatite. In: Bell, K. (Ed.), Carbonatites: Genesis and Evolution. Unwin Hyman, London, pp. 428–447.

Lécuyer, C., Picard, S., Garcia, J.-P., Sheppard, S.M., Grandjean, P., Dromart, G., 2003. Thermal evolution of Tethyan surface waters during the Middle-Late Jurassic: evidence from $\delta^{18}O$ values of marine fish teeth. Paleoceanography 18, 1076.

Malone, M.J., Baker, P.A., Burns, S.J., 1996. Recrystallization of dolomite: an experimental study from 50 to 200 °C. Geochim. Cosmochim. Acta 60, 2189–2207.

Marks, M.A., Neukirchen, F., Vennemann, T., Markl, G., 2009. Textural, chemical, and isotopic effects of late-magmatic carbonatitic fluids in the carbonatite–syenite Tamazeght complex, High Atlas Mountains, Morocco. Mineral. Petrol. 97, 23–42.

McLaughlin, K., Silva, S., Kendall, C., Stuart-Williams, H., Paytan, A., 2004. A precise method for the analysis of $\delta^{18}O$ of dissolved inorganic phosphate in seawater. Limnol. Oceanogr. Methods 2, 202–212.

Melcher, G.C., 1966. The carbonatites of Jacupiranga, Sao Paulo, Brazil. In: Tuttle, O., Gittins, J. (Eds.), Carbonatites. Interscience Publishers, pp. 1361–1382.

Melezhik, V., Bingen, B., Fallick, A., Gorokhov, I., Kuznetsov, A., Sandstad, J., Solli, A., Bjerkgård, T., Henderson, I., Boyd, R., Jamal, D., Moniz, A., 2008. Isotope chemostratigraphy of marbles in northeastern Mozambique: apparent depositional ages and tectonostratigraphic implications. Precambrian Res. 162, 540–558.

Migdisov, A.A., Williams-Jones, A., 2014. Hydrothermal transport and deposition of the rare earth elements by fluorine-bearing aqueous liquids. Mineral. Deposita 49, 987–997.

Moore, M., Chakhmouradian, A.R., Mariano, A.N., Sidhu, R., 2015. Evolution of rare-earth mineralization in the Bear Lodge carbonatite, Wyoming: mineralogical and isotopic evidence. Ore Geol. Rev. 64, 499–521.

Morbidelli, L., Gomes, C., Beccaluva, L., Brotzu, P., Conte, A., Ruberti, E., Traversa, G., 1995. Mineralogical, petrological and geochemical aspects of alkaline and alkaline-carbonate associations from Brazil. Earth-Sci. Rev. 39, 135–168.

Morikiyo, T., Hirano, H., Matsuhisa, Y., 1990. Carbon and oxygen isotopic composition of the carbonates from the Jacupiranga and Catalão I carbonatite complexes, Brazil. Bull. Geol. Surv. Jpn 41, 619–626.

Nadeau, S.L., Epstein, S., Stolper, E., 1999. Hydrogen and carbon abundances and isotopic ratios in apatite from alkaline intrusive complexes, with a focus on carbonatites. Geochim. Cosmochim. Acta 63, 1837–1851.

O'Neil, J.R., Roe, L.J., Reinhard, E., Blake, R., 1994. A rapid and precise method of oxygen isotope analysis of biogenic phosphate. Isr. J. Earth Sci. 43, 203–212.

Pan, Y., Fleet, M.E., 2002. Compositions of the apatite-group minerals: substitution mechanisms and controlling factors. Rev. Mineral. Geochem. 48, 13–49.

Pearce, N., Leng, M., 1996. The origin of carbonatites and related rocks from the Igaliko Dyke Swarm, Gardar Province, South Greenland: field, geochemical and CO-Sr-Nd isotope evidence. Lithos 39, 21–40.

Pearce, N., Leng, M., Emeleus, C., Bedford, C., 1997. The origins of carbonatites and related rocks from the Gronnedal-Ika nepheline syenite complex, South Greenland; CO-Sr isotope evidence. Mineral. Mag. 61, 515–529.

Ray, J., Ramesh, R., 1999. A fluid-rock interaction model for carbon and oxygen isotope variations in altered carbonatites. J. Geol. Soc. India 64, 299–306.

Ray, J.S., Ramesh, R., 2000. Rayleigh fractionation of stable isotopes from a multicomponent source. Geochim. Cosmochim. Acta 64, 299–306.

Ray, J.S., Ramesh, R., 2006. Stable carbon and oxygen isotopic compositions of Indian carbonatites. Int. Geol. Rev. 48, 17–45.

Richet, P., Bottinga, Y., Janoy, M., 1977. A review of hydrogen, carbon, nitrogen, oxygen, sulphur, and chlorine stable isotope enrichment among gaseous molecules. Annu. Rev. Earth Planet. Sci. 5, 65–110.

Santos, R.V., Clayton, R.N., 1995. Variations of oxygen and carbon isotopes in carbonatites: a study of Brazilian alkaline complexes. Geochim. Cosmochim. Acta 59, 1339–1352.

Shemesh, A., Kolodny, Y., Luz, B., 1983. Oxygen isotope variations in phosphate of biogenic apatites, II. Phosphorite rocks. Earth Planet. Sci. Lett. 64, 405–416.

Shemesh, A., Kolodny, Y., Luz, B., 1988. Isotope geochemistry of oxygen and carbon in phosphate and carbonate of phosphorite francolite. Geochim. Cosmochim. Acta 52, 2565–2572.

Suwa, K., Oana, S., Wada, H., Osaki, S., 1975. Isotope geochemistry and petrology of African carbonatites. Phys. Chem. Earth 9, 735–745.

Taylor, H.P., Frechen, J., Degens, E.T., 1967. Oxygen and carbon isotope studies of carbonatites from the Laacher See district, West Germany and the Alnö district, Sweden. Geochim. Cosmochim. Acta 31, 407–430.

Tichomirowa, M., Grosche, G., Götze, J., Belyatsky, B., Savva, E., Keller, J., Todt, W., 2006. The mineral isotope composition of two Precambrian carbonatite complexes from the Kola Alkaline Province—alteration versus primary magmatic signatures. Lithos 91, 229–249.

Trofanenko, J., Williams-Jones, A.E., Simandl, G.J., Migdisov, A.A., 2016. The nature and origin of the REE mineralization in the Wicheeda Carbonatite, British Columbia, Canada. Econ. Geol. 111, 199–223.

Vallée, M., Dubuc, F., 1970. St-Honoré carbonatite complex, Quebec. Can. Min. Metall. Bull. 63, 1384.

Vennemann, T.W., Fricke, H.C., Blake, R.E., O'Neil, J.R., Colman, A., 2002. Oxygen isotope analysis of phosphates: a comparison of techniques for analysis of Ag_3PO_4. Chem. Geol. 185, 321–336.

Wall, F., 2000. Mineral Chemistry and Petrogenesis of Rare Earth-rich Carbonatites With Particular Reference to the Kangankunde Carbonatite, Malawi PhD Thesis University of London.

Wall, F., Niku-Paavola, V., Storey, C., Müller, A., Jeffries, T., 2008. Xenotime-(Y) from carbonatite dykes at Lofdal, Namibia: unusually low LREE: HREE ratio in carbonatite, and the first dating of xenotime overgrowths on zircon. Can. Mineral. 46, 861–877.

Wimmenauer, W., 1966. The eruptive rocks and carbonatites of the Kaiserstuhl, Germany. In: Tuttle, O., Gittins, J. (Eds.), Carbonatites. John Wiley and Sons, New York.

Woolley, A., Kjarsgaard, B., 2008. Carbonatite occurrences of the world: map and database. Geological Survey of Canada open file 5796.

Wyllie, P., 1966. Experimental studies of carbonatite problems: the origin and differentiation of carbonatite magmas. In: Tuttle, O., Gittins, J. (Eds.), Carbonatites. John Wiley and Sons, New York, pp. 311–352.

Yi, H., Balan, E., Gervais, C., Segalen, L., Fayon, F., Roche, D., Person, A., Morin, G., Guillaumet, M., Blanchard, M., et al., 2013. A carbonate-fluoride defect model for carbonate-rich fluorapatite. Am. Mineral. 98, 1066–1069.

Zaitsev, A., Demény, A., Sindern, S., Wall, F., 2002. Burbankite group minerals and their alteration in rare earth carbonatites: source of elements and fluids evidence from C–O and Sr–Nd isotopic data. Lithos 62, 15–33.

Zheng, Y.-F., 1996. Oxygen isotope fractionations involving apatites: application to paleotemperature determination. Chem. Geol. 127, 177–187.